Journal of Power Sources 235 (2013) 280–288

Contents lists available at SciVerse ScienceDirect

Journal of Power Sources

journal homepage: www.elsevier.com/locate/jpowsour

Power production from different types of sewage sludge using microbial fuel cells: A comparative study with energetic and microbiological perspectives

Zhiwei Wang [a,*], Jinxing Ma [a], Yinlun Xu [a,b], Hongguang Yu [a], Zhichao Wu [a]

[a] State Key Laboratory of Pollution Control and Resource Reuse, School of Environmental Science and Engineering, Tongji University, Shanghai 200092, PR China
[b] Department of Civil and Environmental Engineering, Duke University, Durham, NC 27708, United States

HIGHLIGHTS

- Power productions from different sewage sludge were evaluated using MFCs.
- Recovered organic matter (ROM) harvested under anaerobic condition was the best.
- The maximum power output of ROM registered 38.1 W m^{-3}.
- Pyrosequencing revealed the syntrophic community structure on the anodic biofilm.
- Using ROM for power production reduced the negative environmental impacts.

ARTICLE INFO

Article history:
Received 29 December 2012
Received in revised form
6 February 2013
Accepted 11 February 2013
Available online 19 February 2013

Keywords:
Power production
Microbial fuel cell
Sewage sludge
Pyrosequencing
Energy flow analysis

ABSTRACT

Fuel recovery from sewage sludge is a promising energy production method, which can simultaneously address energy issue and environmental concerns associated with waste treatment. This study evaluates power productions from different types of sewage sludge in microbial fuel cells (MFCs) with energetic and microbiological perspectives. Results show that the recovered organic matter (ROM), a kind of anaerobic sewage sludge, is a good candidate for bioelectricity generation compared to conventional waste activated sludge (WAS), giving a maximum power output of 38.1 W m^{-3}. The lower internal resistance of the MFC fed with ROM is attributed to the higher concentration of soluble chemical oxygen demand (SCOD) in the anolyte. At a nominal solid retention time of 8 day, 60.2 ± 4.9% of the total COD in the ROM is removed. The initial chemical composition and microbial consortium in ROM demonstrates the highest exoelectrogenesis potential compared with other WAS samples. The syntrophic communities formed on the surface of anode electrodes enable the successful conversion of the substrates into bioelectricity. Although the recovered energy cannot outweigh the operation costs of the bioelectrochemical systems, the total expenditure for ROM treatment herein is reduced by 30–50% compared to those for WAS.

© 2013 Elsevier B.V. All rights reserved.

1. Introduction

The world is facing an enormous energy challenge. The rising demand for fossil fuels on the one hand shrinks the reserve of the primary energy, and on the other hand, it has raised the concern that the over-consumption with unexpected carbon footprint will lead to an increase in greenhouse gas emission and subsequently global warming [1,2]. As a result, the development of alternative renewable fuel sources and innovative energy production methods, which are potentially carbon neutral, has gained increasing popularity during the last decades [3].

Among various energy production options, fuel recovery from organic waste seems one of the tempting alternatives, probably because this concept simultaneously addresses energy issue and environmental concerns associated with the conventional waste treatment (such as landfill) [4]. Sewage sludge is an abundant organic waste generated in wastewater treatment plants, and presently its management (handling, treatment and disposal) accounts for about 0.6–1.8% of the electrical energy load in developed countries [1,5]. However, prevalent literature has confirmed that in conventional wastewater biological treatment processes, 25–50% energy needs of a plant might be satisfied by using the biogas produced from sewage sludge [6]. Therefore, it is possible to hypothesize that sewage sludge treatment has the prospect to become a net energy producer if the organic biomass serves as biofuel rather than a waste.

* Corresponding author. Tel./fax: +86 (21)65980400.
E-mail address: zwwang@tongji.edu.cn (Z. Wang).

0378-7753/$ – see front matter © 2013 Elsevier B.V. All rights reserved.
http://dx.doi.org/10.1016/j.jpowsour.2013.02.033

Up to now, different technologies have been considered to extract useful energy from sewage sludge, including anaerobic digestion, pyrolysis and bioelectricity generation [3,4,7,8]. Compared to other techniques, bioelectricity generation by using microbial fuel cells (MFCs) is a reliable and promising process since it can convert the chemical energy in the organics directly into useful electricity energy in a compact reactor [9]. Notably, the transfer efficiency of energy from the organics to electricity in MFCs was estimated to be 44%, higher than that (28–40%) with anaerobic treatment [1,10]. Dentel et al. are the first group using sludge for direct generation of electricity [7], and since then, the application of MFCs in energy recovery from sewage sludge has drawn wide attention among the academic community [11–14]. Jiang et al. [11] and Xiao et al. [8,12] reported that a power density of 8.5 W m^{-3} and 0.091–0.292 W m^{-3} from waste activated sludge (WAS) were achieved in two-chamber MFCs, respectively. Further attempts were conducted to improve oxygen transfer at cathodes as well as to reduce the operation cost. Zhang et al. incorporated biocathodes into a three-chamber MFC to yield electricity from WAS, and a maximum power output of 13.2 ± 1.7 W m^{-3} was produced due to the low internal resistance [14].

Nevertheless, current studies are highly focused on improving the cell performance and reducing the material expenditure [11–14], but little attention was paid to the impacts of the substrate they employed on the sustainability of the entire system. The most common sewage sludge, WAS, indeed is an energy-intensive by-product of the aerobic activated sludge process, probably resulting in the fact that the power produced from the WAS is insufficient to satisfy the energy needs for the upstream units [1]. By contrast, the anaerobic sewage sludge (e.g., primary sludge or recovered organic matter [15]) could be harvested in low-energy consuming reactors (e.g., settling tank or dynamic membrane separation reactor [15]). Moreover, anaerobic sewage sludge contains high concentrations of easily biodegradable organic polymers, permitting short hydrolysis and fermentation time [16]. To date, there has been very limited information on comparison of the power production from different types of sewage sludge, especially with respect to assessing the sustainability of the hybrid systems.

The overarching goal of this study is, therefore, to evaluate the power production from three types of sewage sludge in MFCs. The cell performance was further correlated with the characteristics of the sewage sludge using electrochemical impedance spectroscopy, Fourier transform-infrared spectroscopy and 454 high-throughput pyrosequencing. In addition, energy flow analyses were conducted to verify the sustainability of the entire systems, including the MFCs and the upstream units where the sewage sludge was obtained.

2. Materials and methods

2.1. Sewage sludge

Two parallel hybrid systems, located at Quyang wastewater treatment plant (Shanghai, China), were constructed in this study to treat municipal wastewater (Fig. 1). System I aims at energy and resource recovery; an upflow dynamic membrane separation (DMS) reactor was employed to capture the influent organic matter and a low organic loading membrane bioreactor (L-MBR) to improve the quality of the treated wastewater. The other system employing conventional membrane bioreactor (C-MBR) was operated in parallel for comparison. The configuration and operation parameters of the reactors were similar to those mentioned in our previous publications [15,17,18].

The recovered organic matter (ROM), a kind of anaerobic sewage sludge, was harvested from the DMS reactor, and two types of aerobic WAS were collected from L-MBR and C-MBR, respectively (Table 1). The sewage sludge samples were first purged with nitrogen gas, supplied with 50 mM phosphate buffer (19 mM $NaH_2PO_4 \cdot H_2O$ and 31 mM $Na_2HPO_4 \cdot H_2O$) [11], and then stored at 4 °C prior to use. During the experiment, these samples served as the anodic substrates of the MFCs (Table 1). The total chemical oxygen demand (tCOD), soluble chemical oxygen demand (SCOD), total suspended solids (TSS) and volatile suspended solids (VSS) of sludge samples were determined according to the *Standard Methods* [19]. The contents of C and N in the samples were analysed by an elemental detector (Vario EL III, Elementar, Germany). The differences of the raw sewage sludges were not significant at a 0.05 level, in term of tCOD ($p = 0.058$) and VSS ($p = 0.322$).

2.2. MFC configuration and operation conditions

Fig. S1 in the supporting information shows a diagram of the MFC used for power production. The cubic-shape MFC comprised two identical Plexiglas chambers which were separated by a proton exchange membrane (PEM, Nafion™ 117, Dupont Co., U.S.) and pressed up by stainless steel bolts. The cross section of the working area of these two chambers was 100 cm^2, and each chamber had a liquid volume of 500 mL. After electrode material (carbon felt, 1 cm × 1 cm × 4 cm, Junrui Co., China) and Ag/AgCl reference electrode (+197 mV *vs.* standard hydrogen electrode, SHE) were installed, the net volume of anode and cathode chamber decreased to 118 ± 1 mL and 118 ± 2 mL, respectively. External electrical circuit was connected to the electrodes by pushing a graphite rod (6 mm diameter, Nanqiu carbon Co., Shanghai, China) into the carbon felt. Prior to use, the carbon felt and rod were washed in 1 M HCl and 1 M NaOH for 48 h and rinsed with DI water to remove possible trace metal and biomass contamination [20].

In this study, experiments were conducted in semi-continuous mode at 25 ± 2 °C. The sewage sludge was directly used as anodic inoculum and substrate. Half of the anolyte was discharged and replaced with fresh sludge every 4 days to initiate a new cycle, thus maintaining a nominal solid retention time of 8 day. The catholyte was 50 mM $K_3Fe(CN)_6$ aqueous solution in a 100 mM KH_2PO_4 buffer with its pH adjusted to 7 using 1 M NaOH [21]. The anolyte and catholyte were continuously recirculated at a rate of 3 L h^{-1} to keep the liquor well mixed. In order to investigate the impacts of exoelectrogenesis on biomass degradation and microbial community structure, control experiments were also performed using the identical MFCs operated in the same way as mentioned above but under open-circuit mode.

2.3. Analyses and calculations

2.3.1. Electrochemistry analyses

The graphite electrical contacts of both chambers were connected to an external resistor (R_e), and the voltage (U) across R_e in the circuit of the MFCs and the anode potential (E_{pa}) were recorded using a data acquisition system (RBH8251, Ruibohua Co., China) connected to a computer. The current (I) through the electrical circuit was determined from the measured voltage (U) according to $I = U/R_e$.

The polarization curve was performed by a multi-functional electrochemical workstation (CS350, Corrtest Co., China) at a scan rate of 1.0 mV s^{-1}. The power density was calculated based on the net anode chamber volume [9]. The Coulombic efficiency of the cells was determined according to the method reported by Fan et al. [22].

The internal resistance of MFCs was monitored by electrochemical impedance spectroscopy. Impedance measurements were conducted using the multi-functional electrochemical workstation at open circuit voltage over a frequency range of 10^5 to 10^{-2} Hz with

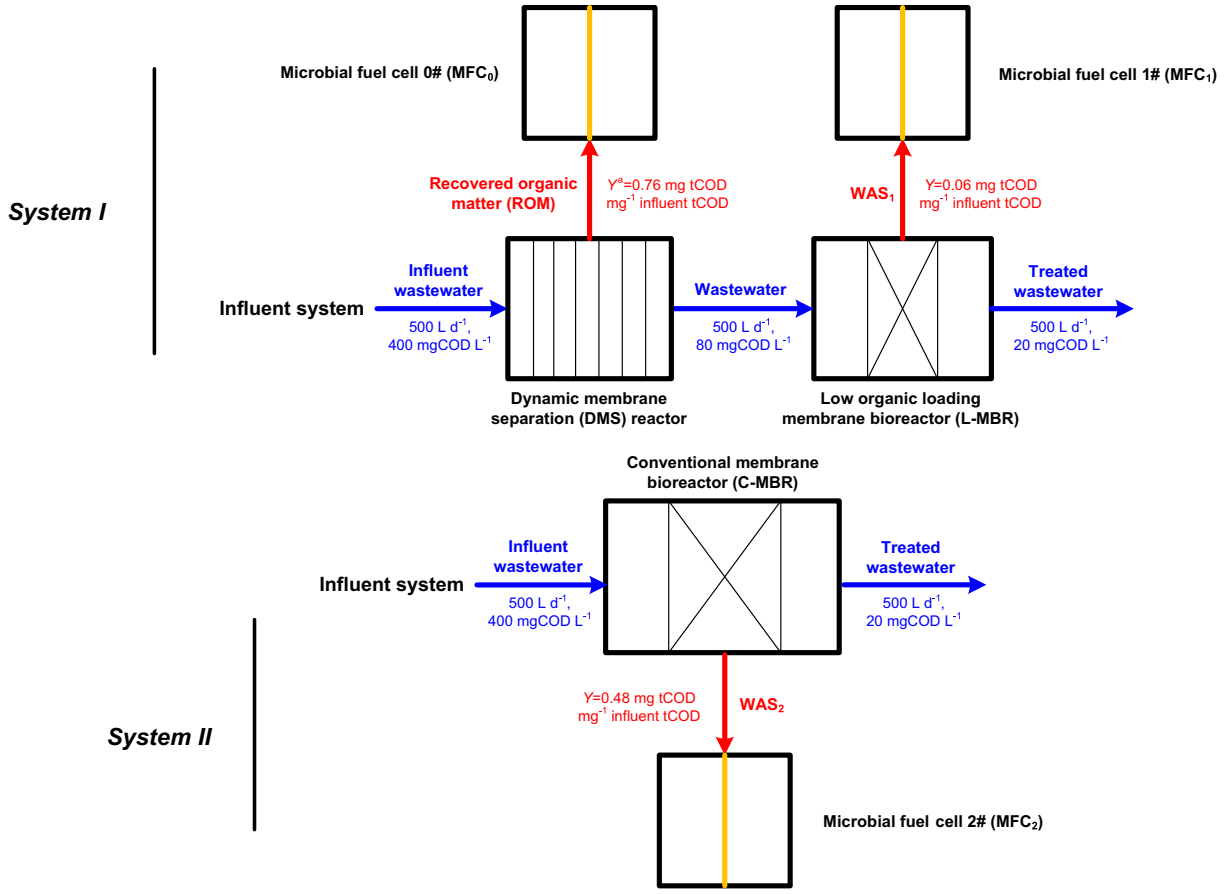

Fig. 1. Schematics of the two parallel hybrid systems. Note: The yield rates (Y) are calculated as follows: $Y = (C_i \times V)/(C_{inf} \times Q)$, where C_i is the tCOD concentration of the sewage sludge (mg L^{-1}), V is the volume of the sewage sludge (L d^{-1}), C_{inf} is the tCOD concentration of the influent wastewater (400 mg L^{-1}), and Q is the wastewater flow rate (L d^{-1}).

a sinusoidal perturbation of 5 mV amplitude. The ohmic resistance and the polarization resistance were calculated from the equivalent circuit of the system [20,23]. The software ZView (Scribner Associates Inc., U.S.) was employed to process and fit the data.

2.3.2. Fourier transform-infrared spectrometry (FT-IR)

The raw sewage sludge (ROM, WAS_1 and WAS_2), the treated anolyte (Tr-MFC_0, Tr-MFC_1 and Tr-MFC_2), the anodic biofilms (Bi-MFC_0, Bi-MFC_1 and Bi-MFC_2) of the MFCs, and the treated sludge from control tests (C-ROM, C-WAS_1 and C-WAS_2) were collected and centrifuged at 6000 rpm for 10 min. Then the sediments were freeze-dried (−40 °C, 48 h), ground, sieved (size fraction of 50–100 mesh) and then stored in a desiccator for further analysis.

FT-IR of the samples was carried out using Nicolet 5700 FT-IR (Thermo Electron, U.S.). KBr tabletting method was employed for sample preparation. The ratio of the sample to KBr was 1:100 and the samples were prepared at a pressure of 30 kPa [24]. Cluster analysis of the spectra using between-groups linkage method was conducted by SPSS software (SPSS Inc., U.S.). Peak assignments for secondary structures were based on the spectral analysis of model peptides and proteins of known structures as documented previously [25].

Table 1
Characteristics of the three types of sewage sludge ($n = 4$).

	Source & destination[a]	tCOD (mg L^{-1})	TSS (g L^{-1})	VSS (g L^{-1})	C/N
ROM	DMS reactor → MFC_0	10,622 ± 940	11.4 ± 0.9	6.4 ± 0.8	9.1 ± 1.9
WAS_1	L-MBR → MFC_1	8109 ± 1122	9.3 ± 0.5	5.6 ± 0.6	5.5 ± 1.8
WAS_2	C-MBR → MFC_2	9034 ± 1655	8.5 ± 0.8	6.0 ± 0.7	5.7 ± 0.4

[a] Source & destination indicate where the sewage sludge was obtained and with which MFCs were fed.

2.3.3. Microbiology analysis

454 high-throughput pyrosequencing was employed to reveal the microbial community structures of the raw sewage sludge (ROM, WAS_1 and WAS_2) and anodic biofilm (Bi-MFC_0, Bi-MFC_1 and Bi-MFC_2) samples. The DNA extraction protocol was the same as that in our previous publication [17], and we normalized the DNA to the same concentration for subsequent amplifying use. Fragments of 16S rRNA gene containing the V4–V5 regions were amplified from the extracted DNA using primer sets (Table S1 in the supporting information). The fused forward primer included a 10-nucleotide barcode inserted between the Life Sciences primer A and the forward primer, which allowed sample multiplexing during the pyrosequencing in a single run.

The individual PCR mixture was prepared in 20 μL volume and contained 0.25 μL of Taq (ExTaq 2.5 U μL^{-1}, Takara, Dalian, China), 2 μL of 10 × buffer (Mg^{2+} free), 2.4 μL of Mg^{2+} (25 mM), 1.6 μL of dNTP mix (2.5 mM each), and 0.4 μL of each primer (10 μM) and 1 μL of the template. Reactions were conducted on a GenAmp PCR System 9700 (Perkin–Elmer Applied Biosystems, Foster City, CA, U.S.) under the following thermocycling steps: 95 °C for 5 min, followed by 25–30 cycles at 94 °C for 30 s, 58 °C for 30 s, 72 °C for 90 s and a final extension step at 72 °C for 10 min. After PCR amplification, the mixture of amplicons was purified using the UNIQ-10 PCR Purification Kit (Sangon, Shanghai, China) and then used for pyrosequencing on a Roche massively parallel

454 GS FLX+ Titanium sequencer (Roche 454 Life Sciences, Branford, CT, U.S.). Following pyrosequencing, Pipeline Initial Process tool in RDP's Pyrosequencing Pipeline were applied to (1) remove sequences containing any ambiguous base calls (Ns); (2) check the completeness of the barcodes and the adaptor; (3) remove sequences shorter than 150 bp [13]. After that, barcodes and primers were trimmed from the resulting sequences, and PCR chimeras were screened for quality as recommended by Haas et al. [26]. Finally, pyrosequencing produced 103,400 high-quality V4-V5 tags of the 16S rRNA-gene with an average length of 408 bp.

Clustering of the operational taxonomic units (OTUs) was initially performed by setting a cutoff of 3% (equivalent to 97% similarity) using the MOTHUR program (http://www.mothur.org/wiki/Main_Page). From the cluster file, rarefaction curves and Shannon index curves were generated in MOTHUR for each sample [27]. Representative sequences from each OTU were assigned down to the phylum, class and genus level using the RDP-II Classifier with a set confidence threshold of 80% [14].

2.3.4. Other calculation procedures

In this study, we employed the carbon felt (1 cm × 1 cm × 4 cm) as the electrode material to facilitate the anodic interface reaction [9]. Inevitably, parts of particulate organic matters were retained by the anodic biofilm, thus "improving" the contaminant removal efficiency. Therefore, we deducted the anodic biofilm yield from the observed tCOD, TSS and VSS removal rate, respectively. The calculation procedures of these parameters were conducted according to Logan et al. [28]. The student's *t*-test was used to compare two data groups, and one way analysis of variance to compare three data groups. SigmaPlot (Version 11.0, Systat Software, Inc., U.S.) was introduced herein to process the data.

3. Results

3.1. Electrochemistry

Initially, the three MFCs were started up with an external resistance of 1000 Ω (Fig. 2), and the output voltages of the cells registered the maximum values of 0.67 V, 0.45 V and 0.63 V after operation for about 100 h. After the R_e was decreased to 100 Ω at the beginning of the second operation cycle (Fig. 2A), the power densities of MFCs sharply increased to 10.1 W m^{-3}, 5.2 W m^{-3} and 13.3 W m^{-3}, respectively. Reproducible cycles ($n = 4$) were obtained with the replenishment of new anolyte every 4 days, giving the highest power densities of 21.4 ± 0.4 W m^{-3}, 5.2 ± 0.1 W m^{-3} and 13.5 ± 0.1 W m^{-3} with the fixed external resistance ($R_e = 100$ Ω). Furthermore, to evaluate the maximum power productions (PD_{max}) from the three types of sewage sludge under the optimal conditions, the polarization curve was performed when the output current reached its local peak (Fig. 3A). In this study, the PD_{max} of the cells were 38.1 W m^{-3}, 11.7 W m^{-3} and 24.0 W m^{-3}, respectively. We observed higher power densities than those reported in other MFC studies using sewage sludge as fuel [8,11,12,14].

The internal resistances of the MFCs were investigated using the electrochemical impedance spectroscopy that has been recently employed to analyse the key factors limiting the cell power output [9]. As verified in prevalent literature [23], the internal resistance of the MFC was comprised of solution resistance (R_{ohm}) and electrode polarization resistance (R_P, including anodic polarization resistance R_a and cathodic polarization resistance R_c). A Warburg element was added herein in parallel to R_a or R_c to represent the diffusion situation. By fitting the experimental data into the equivalent circuits, we obtained the internal resistance compositions of the MFCs (Fig. 3B). It could be observed that the polarization resistance contributed to the majority of the internal resistance, and the internal resistance of MFC_0 was lower than that of MFC_1 or MFC_2.

3.2. Sewage sludge degradation

Fig. 4 demonstrates the degradation of the sewage sludge under different operation modes. Compared to control tests, the tCOD removal rates in MFCs were significantly increased after the circuits were closed. The substrate consumption was further enhanced with the decrease of the external resistance (Fig. 4A). For instance, the average tCOD removal rate of ROM was 2.1% in the control test (open circuit), while it registered a value of 60.2% after the system was loaded with a R_e of 100 Ω. Similar conclusions could be drawn with regard to the hydrolysis of particulate matters, which is in agreement with previous reports of using WAS as fuel of MFCs [12,14]. Notably, ROM was a more biodegradable substrate compared to WAS in lower R_e systems (Fig. 4). More than half of the organic matter in ROM could be mineralized during the 4 days operation but only 47.2% of that was achieved in WAS_1 and WAS_2. The efficient anaerobic metabolism at the anode of MFC_0 also accelerated the hydrolysis of particulate organic matters (Fig. 4C). Nevertheless, a higher electron loss rate was observed in MFC_0. The Coulombic efficiency of the three reactors with R_e of 100 Ω was 18.0 ± 0.6%, 23.8 ± 3.8% and 37.0 ± 6.0%, respectively.

In order to explore the degradation mechanism of sewage sludge, we investigated the chemical components of both raw sludge (ROM, WAS_1 and WAS_2) and degradation products (Tr-MFC_0, Tr-MFC_1 and Tr-MFC_2; C-ROM, C-WAS_1 and C-WAS_2) (Fig. 5A). From the FT-IR

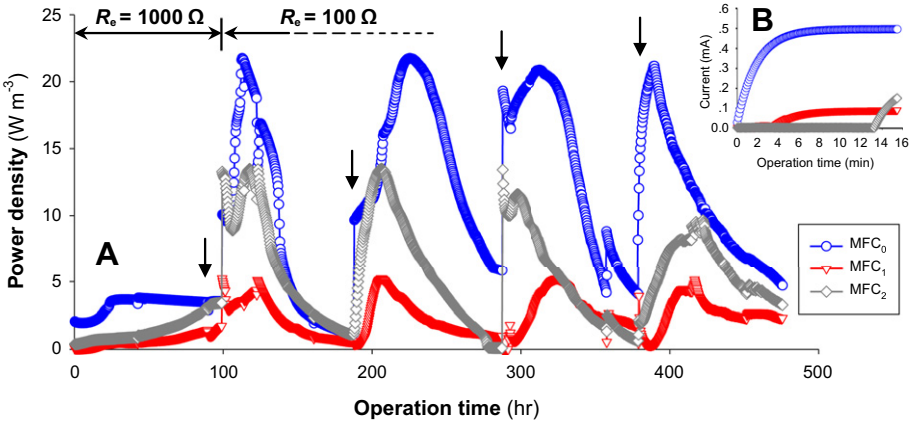

Fig. 2. Variation of power production during the experiments from three types of sewage sludge (arrows indicate the replenishment of anolyte). (A) Power density curves, (B) current curves at the beginning of the operation.

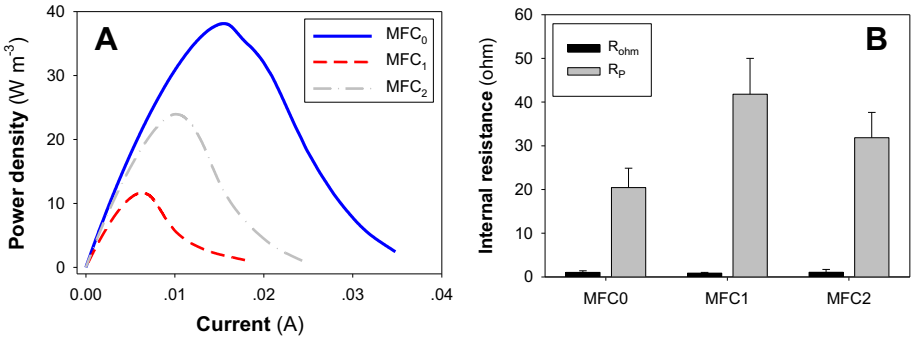

Fig. 3. Electrochemical analyses of the MFCs. (A) Maximum power productions, (B) internal resistance compositions (R_{ohm} and R_p represent the ohm resistance and polarization resistance).

spectra, three categories of organic matters could be well distinguished: aliphatic compounds with methylene groups ($\nu_s CH_2$ at 2950 cm^{-1} and $\delta_s CH_2$ at 1455 cm^{-1}), protein-like substances with carboxyl groups ($\nu_s C{-}O$ at 1385 cm^{-1}) and amides (twin peaks at 1540 and 1650 cm^{-1}), and polysaccharides or polysaccharide-like substances (symmetric and asymmetric C=O stretch at 1000–1200 cm^{-1}) [24,29]. These vibrational signals are ubiquitous in the FT-IR spectra of sludge samples due to the intrinsic characteristics of biomass [25]. During the degradation of sewage sludge, the variation of functional groups was observed. As shown in Fig. 5A, the accumulation of O-acetylated carbohydrates was present in control tests, but did not occur in MFCs. Compared to the initial compounds in the anolyte, the ratio of amide I (–NH_2) to amide II (–NH–) of the metabolic products was increased, which might be attributed to the hydrolysis of peptides and the decomposition of protein-like substances [25]. Moreover, the nine samples could be assigned into three groups at a benchmark of 0.64: (1) Group I includes WAS_2, C-WAS_1 and all degradation products (Tr-MFC_0, Tr-MFC_1 and

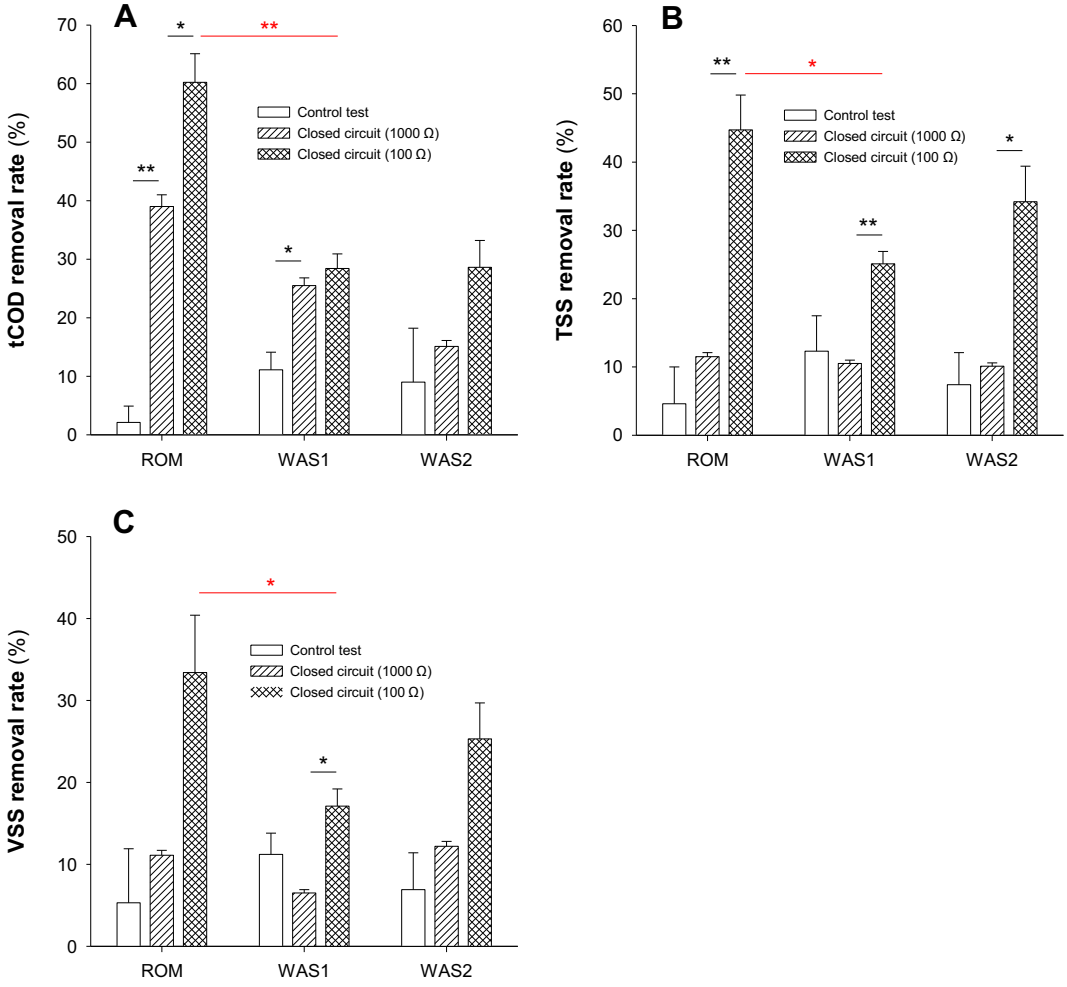

Fig. 4. Comparison of the sewage sludge degradation under different operation modes (control test, open circuit; closed circuit, $R_e = 1000\ \Omega$; closed circuit, $R_e = 100\ \Omega$). (A) tCOD removal rate, (B) TSS removal rate, (C) VSS removal rate. $^{*}p < 0.05$ and $^{**}p < 0.01$ (Student's t-test). Data are representative of at least two independent experiments.

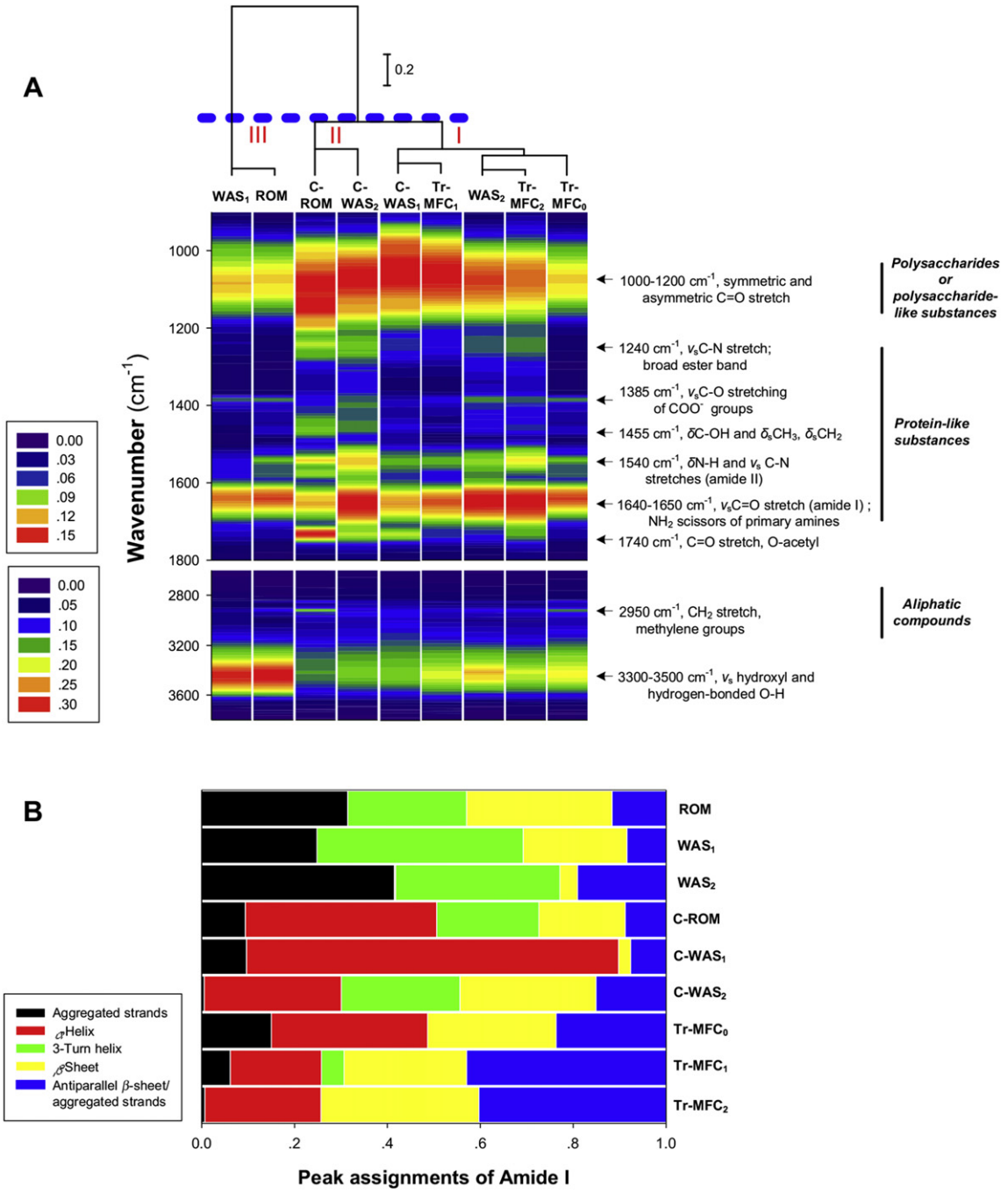

Fig. 5. FT-IR spectra of raw sewage sludge (ROM, WAS_1 and WAS_2) and degradation products (C-ROM, C-WAS_1 and C-WAS_2; Tr-MFC_0, Tr-MFC_1 and Tr-MFC_2) from control tests and MFCs. (A) Hierarchical clustering analysis of the spectra, (B) peak assignments of Amide I. (For interpretation of the references to colour in this figure legend, the reader is referred to the web version of this article.)

Tr-MFC_2) from MFCs; (2) Group II is comprised of two kinds of fermentation products (C-ROM and C-WAS_1); and (3) Group III contains two types of raw sewage sludge, ROM and WAS_1. The hierarchical clustering analysis indicated that in certain treatment process (e.g., fermentation or exoelectrogenesis process), the degradation products (or intermediate products) of sewage sludge could be quite similar with identical functional groups, even though the sludge was of different origins and diverse properties.

Subtle differences in protein secondary structures were interpreted by resolving the amide I region (1600–1700 cm^{-1}) into component peaks using derivative analyses and curve-fitting procedure (Fig. S2 in the supporting information). The peak assignments of amide I are summarized in Fig. 5B. Initially, the raw sewage sludge was mainly comprised of aggregated strands and 3-Turn helix. As the sludge was digested in control tests, aggregated strands (1610–1625 cm^{-1}) with strong infrared absorbance were decreased, and α-Helix (1648–1657 cm^{-1}) became more prevalent than 3-Turn helix (1659–1666 cm^{-1}) probably due to the changes in the inter/intra-molecular hydrogen bonding [30]. The presence of exoelectrogenesis also had an effect on the variations of protein secondary structures; the sheet content (β- and antiparallel β-) was high in Tr-MFC_0, Tr-MFC_1 and Tr-MFC_2.

3.3. Identification of the exoelectrogenic communities

Initially, we obtained 9842-44948 high-quality sequences from the six samples after removing the low quality reads, trimming the barcodes and primers, and filtering out chimeras. To conduct the downstream analyses at the same sequencing depth, each gene library size was normalized to 9842 sequences, i.e., the smallest among the six samples [31]. Details about the richness and diversity of microbial communities could be found in the supporting information (Fig. S3).

In order to identify the exoelectrogenic communities on the anodic biofilms of MFCs, the qualified sequences were then assigned down to the class and genus levels. The average abundances of the most dominant taxa (relative abundance >0.5%) in the anodic biofilm samples (Bi-MFC_0, Bi-MFC_1 and Bi-MFC_2) are demonstrated in Fig. 6, and the grey shadow indicates the variation ranges. In present test, pyrosequencing revealed that *Clostridia* (23.0%), *Betaproteobacteria* (9.1%), *Bacteroidia* (9.0%), *Gammaproteobacteria* (6.7%), and *Holophagae* (3.7%) were the major classes of the microbial communities on the anodic biofilms. This result is comparable to previous investigations of microbial communities existing in the bioelectrochemical systems [13,14]. As shown in Fig. 6, the top three genera on the anodic biofilms included two strains of exoelectrogenic candidates (unclassified_*Clostridiales* and *Clostridium XI*), which exhibited a similarity of 86% with the well-known exoelectrogenic bacterium (*Clostridium butyricum* EG3) [32]. The other phylogenetic group was a new bacterium, accounting for 6.4% of the total genetic information. Notably, many of the predominant genera, involving *Arcobacter* (1.5 ± 1.4%) [33], *Desulfobulbus* (0.8 ± 0.6%) [34], *Desulfovibrio* (0.7 ± 0.5%) [35] and *Geobacter* (0.5 ± 0.2%) [13,36], have been shown to produce electricity in the MFCs. The other abundant strains, including *Oscillibacter*, *Chitinophagaceae* and *Acidobacteria*, are proficient in degrading part of organic matters, such as cellulose and chitin [13,14,17]. Kiely et al. have reported that many of the predominant exoelectrogenic members have limited metabolic versatility, utilizing only certain fermentation end products, whereas the fermentative partners may be incapable of respiration using the anode [37]. It can be inferred that when a complex organic substrate was employed as the anolyte (e.g., ROM and WAS), a syntrophic microbial community would be formed on the anodic biofilm, thus enabling a reciprocal interaction among these partners to successfully convert virtually any substrate into electrical current.

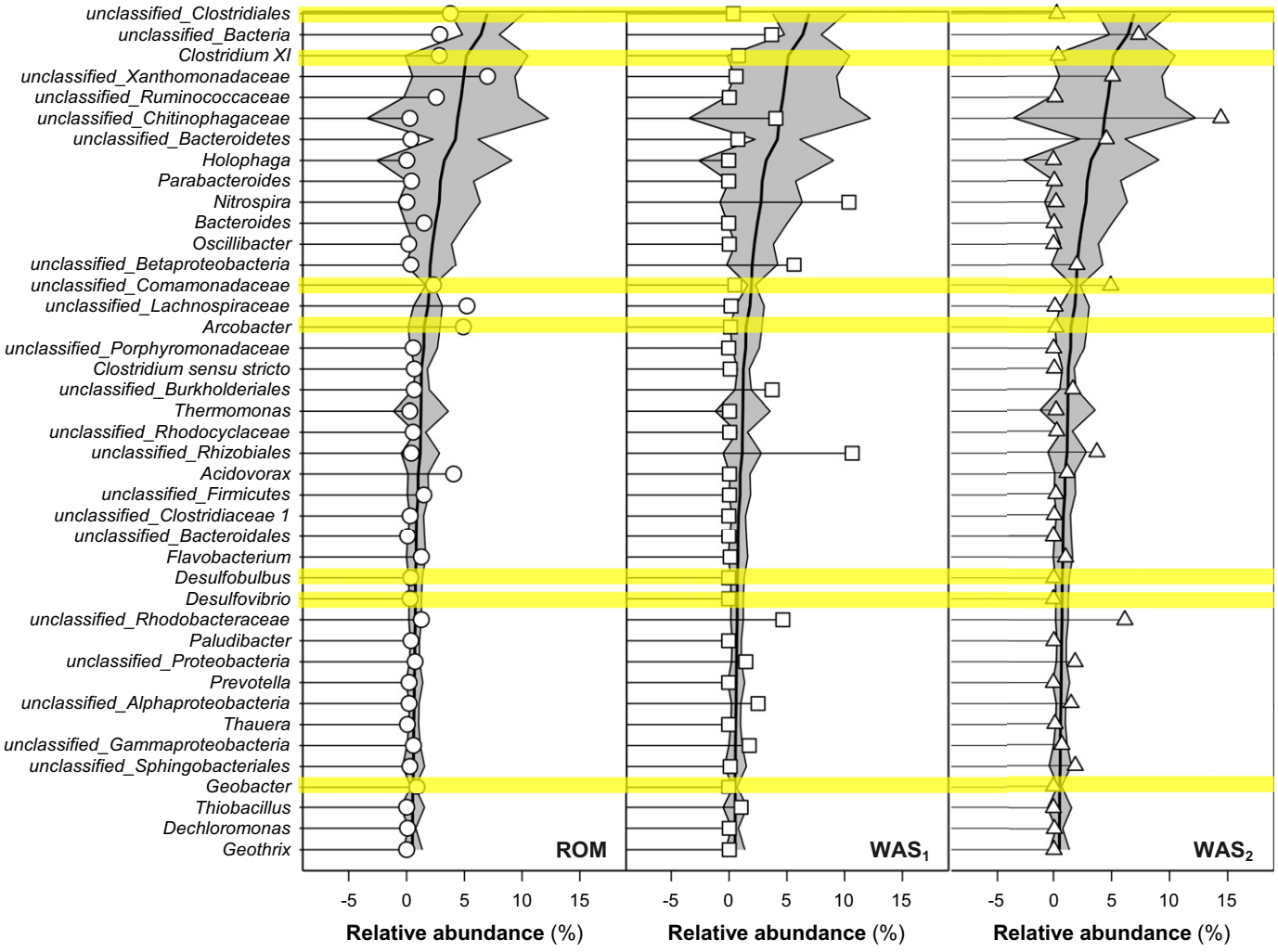

Fig. 6. Average abundances of the most dominant taxa (relative abundance >0.5%) in the anodic biofilm samples (Bi-MFC_0, Bi-MFC_1 and Bi-MFC_2), and their percentages in the three raw sewage sludge samples (ROM, WAS_1 and WAS_2). The vertical black line indicates the average abundances in the biofilm samples and the grey shadow represents the variation ranges. The scatter points show the percentages of the corresponding genera in ROM, WAS_1 and WAS_2, respectively. The horizontal yellow shadow refers to the exoelectrogenic candidates [32–36]. (For interpretation of the references to colour in this figure legend, the reader is referred to the web version of this article.)

To distinguish the initial microbial compositions and to evaluate the impact of these differences on the operation of MFCs, the relative abundances of the corresponding genera in the ROM, WAS_1 and WAS_2 are plotted in Fig. 6. It could be observed that most of the taxa from ROM were covered within the grey shadow, while specific phylogenetic groups exiting in the WAS_1 and WAS_2 (e.g., *Nitrospira*, *Burkholderiales*, *Rhizobiales* and *Rhodobacteraceae*) were washed out during the electrogenesis processes. The OTUs assigned into the seven exoelectrogenic strains accounted for 15.2%, 2.0% and 5.8% of the total sequences in the ROM, WAS_1 and WAS_2, respectively. From a biological perspective, it was possible to conclude that ROM might provide the highest potential for power production, followed by WAS_2 and WAS_1.

4. Discussion

Our results show that bioelectricity could be efficiently produced from ROM by using the MFC technique. At the startup of the bioelectrochemical system, MFC fed with ROM was virtually superior to those with WAS. Especially, it could be noticed that MFC_1 and MFC_2 revealed a transient lag phase at the initial period of the experiment, while the current of MFC_0 began to increase as soon as the operation was started (Fig. 2B). In this study, ROM was collected under the anaerobic conditions with initial oxidation-reduction potential of about − 300 mV, whereas the WAS were harvested in the aerobic tanks. Alternative electron acceptors (e.g., O_2, NO_3^- and SO_4^{2-}) are always abundant in the WAS (WAS_1 and WAS_2), which could induce a competition for electron donors with the anode and subsequently decreased the electron transfer efficiency [38]. Additionally, compared to those in WAS, the microbial community in ROM demonstrated a better biological compatibility with the bioelectrochemical process (Fig. 6), i.e., the initial microbial consortium was fermentative or electrochemical active. That explains why efficient bioelectricity generation was observed even during the inoculation step.

In low R_e bioelectrochemical systems, the highest power density from ROM was 21.4 ± 0.4 W m^{-3}, much higher than those from WAS (WAS_1 and WAS_2). The PD_{max} of MFC_0 registered a value of 38.1 W m^{-3} when the external resistance was set equal to the internal resistance. To the best of our knowledge, power density in MFC studies is always limited by internal resistance as a result of various factors [9,23,28]. In present work, the internal resistances were mainly comprised of the polarization resistances which were correlated with the charge transfer (activation resistance) and concentration losses (diffusion resistance) [23]. At the anode, either a limited discharge of oxidized species from the electrode surface or a limited supply of reduced species towards the electrode would increase the concentration losses [28]. During the experiment, the average SCOD concentration of the anolyte in MFC_0 anode chamber was kept at 519 ± 28 mg L^{-1}, while those of MFC_1 and MFC_2 were 431 ± 44 mg L^{-1} and 464 ± 131 mg L^{-1}, respectively. Thus, it could be concluded that a higher SCOD concentration in the anode chamber might suggest a lower concentration polarization resistance, thus enabling a more satisfied power production from MFC_0. In addition, as revealed in the FT-IR spectra (Fig. 5B), the sheet content (β- and antiparallel β-) of the protein secondary structures were predominant in the anolyte during the MFC operation. This phenomenon probably indicated that in the mixed liquor electron transfer resistance might be reduced with this inter/intra-molecular hydrogen bonding. It could be observed in Fig. 5B that ROM presented the highest sheet content among the three types of raw sewage sludge, which might facilitate electron transfer in the anode chamber.

Apparently, the application of exoelectrogenesis process enha -nced the anaerobic microbial metabolism, which also accelerated the hydrolysis of particulate organic matters and degradation of organic contaminants (Fig. 4). In particular, the intermediate products (e.g., O-acetylated carbohydrates) were accumulated during the anaerobic fermentation. This should be attributed to the fact that under the open-circuit mode the reduced outer membrane cytochromes (or shuttles) could not be efficiently oxidized on the surface of the anode electrodes, subsequently inhibiting the upstream cell respiration [37]. By contrast, the released electrons could be quickly captured by the final acceptors (e.g., $Fe(CN)_6^{3-}$) in low R_e bioelectrochemical systems, which might prevent the accumulation of intermediate products in the anolyte. The efficient reciprocal interaction in the MFC allows the successful conversion of raw sludge into bioelectricity. Moreover, the degradation of ROM were faster than that of WAS in bioelectrochemical systems (Fig. 4). Feng et al. have reported that an increase of substrate C/N ratio would benefit the anaerobic fermentation of complex organics [39], suggesting that the higher C/N ratio of ROM was conducive to the hydrolysis and conversion of organic matters (Table 1). Since the concentration differences of the raw sewage sludge were not significant, the better performance observed in MFC_0 should be mainly attributed to the intrinsic characteristics of ROM.

Energy flows involved in the power production from different sewage sludge were further evaluated with respect to the sustainability of entire systems. The operation expenditure of the upstream units (e.g., DMS, L-MBR and C-MBR) was expressed as the embodied energy consumption for sewage sludge (Fig. 1), and the energy input and output relating to ROM, WAS_1 and WAS_2 in bioelectrochemical systems are listed in Table 2. For comparison, the units of energy flow were normalized to the energy consumption (or recovery) in the treatment of one kilogram biomass (i.e., kWh kg^{-1}). As shown in Table 2, 0.689 kWh kg^{-1}, 0.223 kWh kg^{-1} and 0.435 kWh kg^{-1} could be extracted from ROM, WAS_1 and WAS_2 by using the MFC technique. Notably, positive environmental impacts arising from MFC_0 fed with ROM were much more significant than those with WAS, as evidenced by the fact that the total energy consumption for ROM treatment in the bioelectrochemical system was 2.87 kWh kg^{-1}, only half of that for the WAS_2 (5.64 kWh kg^{-1}). Moreover, in the DMS reactor 95% of the retained COD were condensed and converted to ROM for bioelectricity generation. Since a larger proportion of influent organic matters were collected for exoelectrogenesis in System I (Fig. 1), the inevitable CO_2 emission without energy recovery was decreased during the wastewater treatment. The present study reveals that utilizing the anaerobic sewage sludge (i.e., ROM) for power production could not only facilitate the exoelectrogenesis process but decrease the negative environmental impacts associated with waste treatment. Nevertheless, it should be noticed that the energy recovered from the exoelectrogenesis process was far from offsetting the operation consumption of the bioelectrochemical systems, let alone the embodied energy from the upstream treatment. The predicament might be partly attributed to the insufficient reoxidation of $K_3Fe(CN)_6$ by oxygen [28], which requires the regular replacement of the catholyte and substantial consumption expenditure (Table 2). In this study, the Coulombic efficiency and power density from ROM and WAS were comparable with relevant literature [11,12,14], but the recovered energy only accounted for 10–20% of the theoretical calorific value of the biomass [1], indicating the substantial opportunity for future improvements by appropriate material selection and development. Furthermore, the hybrid process (System I, Fig. 1) should be improved to develop a more cost-effective application for municipal wastewater and sludge treatment. For instance, future attempts could be considered to combine the ROM separation process and exoelectrogenesis process within one compact reactor. Alternative pretreatment methods are also needed to facilitate the biomass degradation and to reduce the expenditure for residual disposal.

Table 2
Energy flow analyses of the bioelectrochemical systems.

Items	System I						System II		
	ROM			WAS_1			WAS_2		
	Unit	Content	Value kWh kg^{-1}	Unit	Content	Value kWh kg^{-1}	Unit	Content	Value kWh kg^{-1}
Embodied energy consumption	Influent system	Pumps, controls, etc.	0.056	–	–	–	Influent system	Pumps, controls, etc.	0.056
	DMS reactor	Pumps	0.218	L-MBR	Pumps	0.218	C-MBR	Pumps	0.429
		Reagent[a]	0.400		Aeration	0.930		Aeration, stirrers	2.430
		Membrane cleaning	~0.003		Membrane cleaning	~0.003		Membrane cleaning	0.006
Total	0.056 + (0.218 + 0.400 + 0.003) = **0.677**			(0.218 + 0.930 + 0.003) = **1.151**			0.056 + (0.429 + 2.430 + 0.006) = **2.921**		
Operation energy consumption	MFC_0	Pumps	0.369	MFC_1	Pumps	0.369	MFC_2	Pumps	0.369
		Reagent	1.139		Reagent	1.139		Reagent	1.139
		Residual disposal[b]	1.378		Residual disposal	1.866		Residual disposal	1.644
Total	(0.369 + 1.139 + 1.378) = **2.886**			(0.369 + 1.139 + 1.866) = **3.374**			(0.369 + 1.139 + 1.644) = **3.152**		
Energy recovery	MFC_0		0.689	MFC_1		0.223	MFC_2		0.435
Total	**0.689**			**0.223**			**0.435**		

[a] Energy consumption of the reagent was calculated as the reagent expenditure divided by the price of electricity.
[b] Sludge incineration was considered for the residual disposal. The total operation energy consumption (including energy consumption, reagent expenditure, etc.) is about 2.5 kWh kg^{-1} biomass according to prevalent data.

5. Conclusion

In this study, power productions from different types of sewage sludge were evaluated with energetic and microbiological perspectives. The results showed that ROM was a more biodegradable substrate compared to WAS in lower R_e systems, and 60.2% of the organics in the ROM could be removed during 4-day operation. The high SCOD concentration in the anode chamber of MFC_0 was conducive to the electron transfer in the anolyte, which probably accounted for the low polarization resistance and high power density (21.4 ± 0.4 W m^{-3}). FT-IR spectra and 454 pyrosequencing revealed that syntrophic microbial communities were formed on the anodic biofilms, thus preventing the accumulation of intermediate products and enabling the successful conversion of the substrates into bioelectricity. The initial chemical composition and microbial consortium in ROM demonstrated the highest exoelectrogenesis potential, as demonstrated by the efficient power production in MFC_0 even during the inoculation step. Moreover, the total expenditure for ROM treatment was reduced by 30–50% compared to those for WAS through energy flow analysis, although the recovered energy could not satisfy the operation consumption of the bioelectrochemical systems. It is possible to conclude that utilizing ROM for power production could not only facilitate the exoelectrogenesis process but decrease the negative environmental impacts associated with waste treatment.

Acknowledgements

This work was financially supported by the Sino-French Scientific and Technological Cooperation Project in the Domain of Water (2011DFA90400), STCSM Project (12230707000) and the Fundamental Research Funds for the Central Universities.

Appendix A. Supplementary data

Supplementary data related to this article can be found at http://dx.doi.org/10.1016/j.jpowsour.2013.02.033.

References

[1] P.L. McCarty, J. Bae, J. Kim, Environ. Sci. Technol. 45 (2011) 7100–7106.
[2] J. Hill, E. Nelson, D. Tilman, S. Polasky, D. Tiffany, Proc. Natl. Acad. Sci. U. S. A. 103 (2006) 11206–11210.
[3] P. Manara, A. Zabaniotou, Renew. Sustain. Energy Rev. 16 (2012) 2566–2582.
[4] Y.C. Cao, A. Pawlowski, Renew. Sustain. Energy Rev. 16 (2012) 1657–1665.
[5] C.V. Andreoli, M.V. Speling, F. Fernandes, Sludge treatment and disposal, in: Biological Wastewater Treatment Series, vol. 6, IWA Publishing, London, 2007.
[6] EPA Office of Water, Wastewater Management Fact Sheet, Energy Conservation, Environmental Protection Agency, Washington DC, 2006.
[7] S.K. Dentel, B. Strogen, P. Chiu, Water Sci. Technol. 50 (2004) 161.
[8] Z.W. Wang, X.J. Mei, J.X. Ma, Z.C. Wu, Chem. Eng. Technol. 35 (2012) 1733–1743.
[9] B.E. Logan, Microbial Fuel Cells, John Wiley & Sons, Inc., New York, 2008.
[10] Eastern Research Group, Opportunities for and Benefits of Combined Heat and Power at Wastewater Treatment Facilities, Environmental Protection Agency, Washington DC, 2007.
[11] J.Q. Jiang, Q.L. Zhao, J.N. Zhang, G.D. Zhang, D.J. Lee, Bioresour. Technol. 100 (2009) 5808–5812.
[12] B.Y. Xiao, F. Yang, J.X. Liu, J. Hazard. Mater. 189 (2011) 444–449.
[13] L. Lu, D.F. Xing, N.Q. Ren, Water Res. 46 (2012) 2425–2434.
[14] G.D. Zhang, Q.L. Zhao, Y. Jiao, K. Wang, D.J. Lee, N.Q. Ren, Water Res. 46 (2012) 43–52.
[15] J.X. Ma, Z.W. Wang, Y.L. Xu, Q.Y. Wang, Z.C. Wu, A. Grasmick, Chem. Eng. J. 219 (2013) 190–199.
[16] Q. Yuan, M. Baranowski, J.A. Oleszkiewicz, Chemosphere 80 (2012) 445–449.
[17] J.X. Ma, Z.W. Wang, Y. Yang, X.J. Mei, Z.C. Wu, Water Res. 47 (2013) 859–869.
[18] Q.Y. Wang, Z.W. Wang, Z.C. Wu, X.M. Han, Chem. Eng. J. 172 (2011) 929–935.
[19] APHA, Standard Methods for the Examination of Water and Wastewater, twenty-second ed., American Public Health Association/American Water Works Association/Water Environment Federation, Washington DC, 2012.
[20] X.X. Cao, X. Huang, P. Liang, K. Xiao, Y.J. Zhou, X.Y. Zhang, B.E. Logan, Environ. Sci. Technol. 43 (2009) 7148–7152.
[21] P. Aelterman, K. Rabaey, H.T. Pham, N. Boon, W. Verstraete, Environ. Sci. Technol. 40 (2006) 3388–3394.
[22] Y.Z. Fan, H.Q. Hu, H. Liu, J. Power Sources 171 (2007) 348–354.
[23] Z. He, F. Mansfeld, Energy Environ. Sci. 2 (2009) 215–219.
[24] Z.W. Wang, Z.C. Wu, S.J. Tang, Water Res. 43 (2009) 2504–2512.
[25] A.R. Badireddy, S. Chellam, P.L. Gassman, M.H. Engelhard, A.S. Lea, K.M. Rosso, Water Res. 44 (2010) 4505–4516.
[26] B.J. Haas, D. Gevers, A.M. Earl, M. Feldgarden, D.V. Ward, G. Giannoukos, D. Ciulla, D. Tabbaa, S.K. Highlander, E. Sodergren, B. Methe, T.Z. DeSantis, J.F. Petrosino, R. Knight, B.W. Birren, Genome Res. 21 (2011) 494–504.
[27] P.D. Schloss, S.L. Westcott, T. Ryabin, J.R. Hall, M. Hartmann, E.B. Hollister, R.A. Lesniewski, B.B. Oakley, D.H. Parks, C.J. Robinson, J.W. Sahl, B. Stres, G.G. Thallinger, D.J. Van Horn, C.F. Weber, Appl. Environ. Microbiol. 75 (2009) 7537–7541.
[28] B.E. Logan, B. Hamelers, S. Rozendal, U. Schroder, J. Keller, S. Freguia, P. Aelterman, W. Verstraete, K. Rabaey, Environ. Sci. Technol. 40 (2006) 5181–5192.
[29] J.Q. Jiang, Q.L. Zhao, L.L. Wei, K. Wang, Water Res. 44 (2010) 2163–2170.
[30] B.H. Stuart, Infrared Spectroscopy: Fundamentals and Applications, John Wiley & Sons, Inc., Chichester, 2004.
[31] T. Zhang, M.F. Shao, L. Ye, ISME J. 6 (2012) 1137–1147.
[32] B.E. Logan, Nat. Rev. Microbiol. 7 (2009) 375–381.
[33] V. Fedorovich, M.C. Knighton, E. Pagaling, F.B. Ward, A. Free, I. Goryanin, Appl. Environ. Microbiol. 75 (2009) 7326–7334.
[34] D.E. Holmes, D.R. Bond, D.R. Lovley, Appl. Environ. Microbiol. 70 (2004) 1234–1237.
[35] F. Zhao, N. Rahunen, J.R. Varcoe, A. Chandra, C. Avignone-Rossa, A.E. Thumser, R.C.T. Slade, Environ. Sci. Technol. 42 (2008) 4971–4976.
[36] D.R. Bond, D.E. Holmes, L.M. Tender, D.R. Lovley, Science 295 (2002) 483–485.
[37] P.D. Kiely, J.M. Regan, B.E. Logan, Curr. Opin. Biotechnol. 22 (2011) 378–385.
[38] J.M. Morris, S. Jin, Chem. Eng. J. 153 (2009) 127–130.
[39] L.Y. Feng, Y.G. Chen, X. Zheng, Environ. Sci. Technol. 43 (2009) 4373–4380.